

$$a = (2R_1 x)^{1/2}, \quad b = (2R_2 x)^{1/2},$$

$$S(x) = \pi ab = 2\pi(R_1 R_2)^{1/2} x.$$

Then $F(k)$ for large k varies as k^{-2} and $|F(k)|^2$ as k^{-4} . For other kinds of singular points the

asymptotic dependence can change, consequently, the scattered intensity for large k in one, two, and three dimensions varies, respectively, as k^{-2} , k^{-3} , and k^{-4} for contours and surfaces without singularities.

¹N. Bloembergen, *Nonlinear Optics* (Benjamin, New York, 1965).

²I. Freund, *Phys. Rev. Letters* **21**, 1404 (1968).

³G. Dolino, J. Lajzerowicz, and M. Vallade, *Solid State Commun.* **7**, 1005 (1969).

⁴G. Dolino, J. Lajzerowicz, and M. Vallade, *Phys. Rev. B* **2**, 2194 (1970).

⁵R. C. Miller, *Phys. Rev.* **134**, A1313 (1964).

⁶D. A. Kleinman, *Phys. Rev.* **128**, 1761 (1962).

⁷D. A. Kleinman, A. Ashkin, and G. D. Boyd, *Phys. Rev.* **145**, 338 (1966).

⁸A. Guinier and G. Fournet, *Small Angle Scattering of X-Rays* (Wiley, New York, 1955).

⁹L. Schwartz, *Méthodes Mathématiques pour les Sciences Physiques* (Herman & Cie, Paris, 1965).

¹⁰E. Fatuzzo and W. J. Merz, *Ferroelectricity* (North-Holland, Amsterdam, 1967).

¹¹H. Vogt, H. Happ, and H. F. Hafele, *Phys. Status*

Solidi **1a**, 439 (1970).

¹²A. Blanc-Lapierre and R. Fortet, *Théorie des fonctions Aléatoires* (Masson, Paris, 1953), p. 189.

¹³G. Dolino, J. Lajzerowicz, and M. Vallade, *International Conference on Light Scattering in Solids* (Flammarion, Paris, 1971), p. 439.

¹⁴F. Jona and G. Shirance, *Ferroelectrical Crystals* (McMillan, New York, 1962).

¹⁵A. W. Smith, *Appl. Opt.* **3**, 147 (1964).

¹⁶A. G. Chynoweth and J. L. Abel, *J. Appl. Phys.* **30**, 1073 (1959).

¹⁷A. S. Sonin and V. S. Suvorov, *Fiz. Tverd. Tela* **10**, 1031 (1968) [*Sov. Phys. Solid State* **10**, 814 (1968)].

¹⁸F. Moravets and V. P. Konstantinova, *Kristallogr.* **13**, 284 (1968) [*Sov. Phys. Crist.* **13**, 221 (1968)].

¹⁹A. Erdeleyi, *J. Soc. Ind. Appl. Math.* **3**, 17 (1955).

²⁰A. Papoulis, *Systems and Transforms with Applications to Optics* (McGraw-Hill, New York, 1968).

Generalized Random-Walk Model for Singlet-Exciton Energy Transfer*

Zoltán G. Soos[†] and Richard C. Powell[‡]

Sandia Laboratories, Albuquerque, New Mexico 87115

(Received 23 July 1971; revised manuscript received 2 June 1972)

The usual model for singlet-exciton motion and trapping in molecular crystals is generalized to arbitrary finite trapping regions about each activator and to more than nearest-neighbor steps by the random walker. The properties of extended trapping regions, which simulate activator-induced host traps, are obtained rigorously by applying general results for three-dimensional random walks. The capacity $C(A)$ of the extended trapping region is shown, by explicit calculations for a simple cubic lattice, to depend on the size and shape of the trapping region and on the anisotropy and step distribution of the random walker. The capacity controls the competition between singlet-exciton absorption (trapping and subsequent trap fluorescence) and emission (host fluorescence) observed in doped organic crystals. The model accounts qualitatively for the "anomalous" time dependence of the energy-transfer rate in tetracene-doped anthracene and in anthracene- or tetracene-doped naphthalene. The model also accounts for the reported variations in the apparent exciton hopping time, which provide strong evidence for the hypothesis of extended trapping regions.

I. INTRODUCTION

Both exciton diffusion^{1,2} and long-range resonant transfer^{3,4} (LRRT) describe the motion of singlet excitations in molecular crystals. LRRT has been thoroughly documented for energy transfer between immobile excitations on impurities embedded in the crystal. Simpson⁵ demonstrated singlet-exciton diffusion in anthracene and Trlifaj² related theoretically the diffusion constant to the efficient LRRT between adjacent host sites. In the following, we reserve "diffusion" for nearest-neighbor ran-

dom walking by whatever mechanism of the singlet excitation.

Powell and Kepler⁶⁻¹¹ (PK) recently observed the time evolution of both sensitizer (host) and activator (trap) fluorescence in doped organic crystals. Singlet-exciton motion in either crystalline anthracene or naphthalene, the two hosts studied by PK, is generally thought to be diffusional at room temperature, where the shallow host traps which are observed at low temperature are thermally detrapped. The PK data nevertheless decisively rule out the usual formulation of exciton

diffusion and require a fundamental reexamination of singlet-exciton motion in organic crystals at room temperature. Proposals for explaining the time-resolved fluorescence-spectroscopy results have ranged from radiative reabsorption¹² to the usual model for random walks,¹³ to LRRT to the traps,¹¹ to either shallow or deep-host traps,¹⁴ and to thermal detrapping from host traps.¹⁵ As shown recently,¹⁶ *all* these proposals can be ruled out by considering the wealth of experimental data collected by PK.⁶⁻¹¹ For example, the postulate¹⁵ of uncontrollable shallow host traps and thermal detrapping fits the observed time dependence for the rate of energy transfer. But random host traps are implausible¹⁶ in view of the similar observed results in differently prepared crystals^{7,9} with widely different structural and chemical purity.

It is not our purpose here to review the extensive theoretical literature on exciton migration and energy transfer in organic solids.¹⁷ Even the most successful models, such as exciton diffusion or LRRT between fixed impurities, are extensively parametrized theories which are at best consistent with a variety of experimental data. Unambiguous experimental checks have been rare. The PK experiments, for example, provide a clear-cut rejection for the usual formulation of exciton diffusion and trapping and even of the theoretical modifications¹²⁻¹⁵ proposed to account for the time-resolved fluorescence spectroscopy results.

Since singlet-exciton diffusion in anthracene and naphthalene is consistent with many experimental observations at room temperature, we focus on random-walk models for singlet-exciton motion and trapping. Rudemo¹⁸ has discussed rigorously the mathematically simplest model for exciton trapping, when trapping occurs on the first visit by the random walker to an activator site. In this approximation, all activators trap in the same fashion. As shown in Sec. IIIB, however, previously reported fluorescence quenching experiments^{19,20} clearly indicate that different activators in naphthalene quench quite differently. It is therefore not surprising that the direct application¹³ of this random-walk model for trapping fails¹⁶ to account for the PK data. Another simplification usually adopted is that the LRRT distribution of step lengths can be approximated by nearest-neighbor steps. The exciton-diffusion constant² is, in fact, dominated by the rapid nearest-neighbor steps. But the PK data involve energy transfer to randomly distributed isolated activator molecules. As shown below, occasional long steps are then by no means negligible. The usual model for exciton trapping and motion thus contains serious oversimplifications in the interests of mathematical simplicity.

Recent developments in the theory of random

walks by Spitzer,²¹ Rudemo,¹⁸ and Montroll and Weiss²² permit a more realistic model for exciton trapping and motion. We develop here a generalized random-walk model for exciton trapping and motion and apply it to the time-resolved fluorescence spectroscopy results of Powell and Kepler.⁶⁻¹¹

The generalized random-walk model is introduced in Sec. II. To simulate activator-induced host traps²³ which can interrupt briefly the random walk and lead to LRRT to the activator, we introduce an arbitrary finite trapping region about each activator and define trapping to occur on the first visit to an activator site or to one of the activator-induced host traps. The emission (host fluorescence) probability obtained by Rudemo¹⁸ is generalized to extended trapping regions. In Sec. II B we introduce a simple cubic lattice and use the Green's functions tabulated by Maradudin *et al.*²⁴ to obtain numerical results for nearest-neighbor random walks with axial anisotropy and different extended trapping regions. The effects on long steps are discussed in Sec. II C, together with numerical results for a simple cubic lattice.

The connection between the generalized model and the PK data is discussed in Sec. III. The rate of energy transfer $k(t)$ is obtained numerically in Sec. III A from previously published PK data for several tetracene-doped anthracene crystals and for anthracene- or tetracene-doped naphthalene crystals. Experimental evidence for extended trapping regions in naphthalene is presented in Sec. III B from fluorescence-quenching data. It is shown that the generalized random-walk model is consistent with the PK data, but only qualitative comparisons are offered for the monoclinic anthracene and naphthalene crystals, since the quantitative results in Sec. II are based on a cubic lattice.

We thus show that the generalized model is *consistent* with the PK data, but not that random walks provide the *only* model for singlet-exciton energy transfer at room temperature in doped organic crystals. Nevertheless, in our opinion excitonic random walks provide the most complete and consistent model for high-temperature energy transfer. The present work demonstrates that the failure of the usual formulation of exciton diffusion is due to serious oversimplifications of the trapping mechanism and of the exciton motion. Time-resolved fluorescence spectroscopy results may thus provide experimental information about the mechanism of singlet-exciton trapping.

II. GENERALIZED MODEL

Neither direct trap excitation nor trap saturation is important in the PK experiment,⁶⁻¹¹ since there are very few activators and even fewer excitons.

We therefore focus on the properties of a single singlet exciton. The activators (traps) are assumed to be randomly distributed substitutional impurities with density n_T in the sensitizer (host) lattice. The lattice points $\{\vec{R}_n\}$ or an infinite host crystal then define the location of both activators and sensitizers. The random walk of an exciton on the host lattice can terminate with either emission (host fluorescence) or with absorption (trapping and subsequent trap fluorescence). A constant emission probability $\gamma \ll 1$ is assumed before each step to describe host fluorescence.

The first step in constructing a mathematical model for the competition between emission and absorption is to define the random walk on the host lattice. The transition probabilities $P(\vec{a}) \geq 0$ for single steps of $\vec{a} = \vec{R}_i - \vec{R}_j$ specify the random walk. We consider only symmetric random walks with $P(-\vec{a}) = P(\vec{a})$. The normalization condition

$$\sum_{\vec{a}} P(\vec{a}) = 1 \quad (1)$$

expresses the conservation of the singlet exciton. In an infinite periodic lattice with a single site per unit cell, the Green's function^{22,24} $G(\vec{a})$

$$G(\vec{a}) = \frac{1}{(2\pi)^3} \iiint_{-\pi}^{\pi} \frac{e^{i\vec{a}\cdot\vec{r}} d^3r}{1 - \lambda(\vec{r})} \quad (2)$$

corresponds to the expected number of visits to the lattice point \vec{a} by a random walker starting at the origin. The structure function²² $\lambda(\vec{r})$ is defined by

$$\lambda(\vec{r}) = \sum_{\vec{s}} P(\vec{s}) e^{i\vec{s}\cdot\vec{r}}. \quad (3)$$

$\lambda(\vec{r})$ is real for symmetric random walks and reduces to Eq. (1) for $\vec{r} = 0$. Montroll²⁵ has discussed the Green's function for periodic lattices with two molecules per unit cell, but this generalization will not be used here.

The second step in constructing a model is to define the trapping mechanism. The simple definition of trapping on the first visit to an activator site is, as already discussed, inadequate. The definition of trapping adopted in this paper is that the random walk terminates by absorption on the first visit to an arbitrary finite set of $A+1$ lattice points, called the extended trapping region, which contain the activator site and A host sites related to the activator by the translations $\vec{R}(A)$. The random walker then sees a randomly distributed set of identical trapping clusters. The requirement $n_T(A+1) \ll 1$ ensures both long random walks on the average before absorption and negligible overlap between adjacent clusters. The lattice vectors $\vec{R}(A)$ defining the extended trapping region are otherwise arbitrary.

A. Extended Trapping Regions

We begin by neglecting emission ($\gamma = 0$) and applying Spitzer's²¹ general analysis of three-dimen-

sional random walks to absorption by extended trapping regions. A freshly created exciton at \vec{R}_n at $t=0$ is immediately trapped if \vec{R}_n or $\vec{R}_n - \vec{R}(A)$ is an activator site. The initial trapping probability is thus $n_T(A+1)$, since each lattice point has an *a priori* probability n_T of being an activator site. The exciton is trapped after each step, say to \vec{R}_j , if \vec{R}_j or $\vec{R}_j - \vec{R}(A)$ is an activator. Instead of extended trapping regions about each activator, we can therefore think of the exciton sampling, on each step, $A+1$ lattice points related to the extended trapping region by an inversion.

We define the random variable $C_n(A)$ to be the total number of *distinct* lattice points sampled up to and including the n th step. Since the random walk terminates by absorption the first time that \vec{R}_j or $\vec{R}_j - \vec{R}(A)$ is an activator, all random walks containing at least $n+1$ steps will sweep out $C_n(A)$ lattice points which contain *no* traps at all. The probability of absorption on the n th step is

$$p_n = n_T [C_n(A) - C_{n-1}(A)] \quad (4)$$

and is simply n_T times the number of lattice points sampled for the *first* time on the n th step.

It is important to realize that $C_n(A)$ depends on the size and shape of the extended trapping region, but not on the trap density. In particular, $C_n(A)$ is well defined even for $n_T = 0$, when as indicated in Eq. (4) there is no absorption at all. Physically, we might associate different extended trapping regions with different activators. The random variable $C_n(A)$ then does not depend on the activator density, provided only that $n_T(A+1) \ll 1$.

Spitzer²¹ shows that the limit

$$\lim_{n \rightarrow \infty} C_n(A)/n = C(A) \quad (5)$$

exists with certainty and defines the capacity $C(A)$ of the finite subset which is here associated with the extended trapping region. Equation (5) holds for arbitrary three-dimensional transition probabilities $P(\vec{a})$ with finite second moment and arbitrary finite extended trapping regions. Although numerical estimates of $C(A)$ will require specific random walks on specific lattices, the existence of the capacity is a *general* result for three-dimensional random walks. $C(A)$ can be related²¹ to the Green's functions $G(\vec{R}_i, \vec{R}_j)$ which gives the expected number of visits to \vec{R}_j for a random walker starting at \vec{R}_i . The evaluation of $G(\vec{R}_i, \vec{R}_j) = G(|R_i - R_j|)$ for a periodic lattice with a single site per unit cell reduces to evaluating the integral in Eq. (2). The $(A+1) \times (A+1)$ matrix $G(\vec{R}_i, \vec{R}_j)$, with i and j ranging over the $A+1$ sites of the extended trapping region, is readily constructed once the Green's functions are known. The capacity $C(A)$ is given by the sum of the elements of the inverse matrix $G^{-1}(\vec{R}_i, \vec{R}_j)$.²¹

Spitzer²¹ also found in general how $C_n(A)/n$ ap-

proaches $C(A)$ for an isotropic random walk with

$$\sigma^2 = \sigma_j^2 = \sum_{\vec{a}} (a_j)^2 P(\vec{a}), \quad j = x, y, z \quad (6)$$

and $P(\vec{a}) = P(|a|)$. The asymptotic result is

$$C_n(A) - C_{n-1}(A) = C(A) \left(1 + \frac{2C(A)}{(2\pi\sigma^2)^{3/2}} \frac{1}{n^{1/2}} + \dots \right), \quad (7)$$

with corrections of order n^{-1} . This result holds in general for isotropic three-dimensional random walks and finite extended trapping regions. In particular, the only requirement on the distribution of step lengths is that the second moment $\sigma_x^2 + \sigma_y^2 + \sigma_z^2$ be finite. Montroll and Weiss²² have obtained the anisotropic analog to Eq. (7) for the special case $A=0$ when absorption requires an actual visit to a trapping site; their result is to replace $(\sigma^2)^{3/2}$ by $\sigma_x\sigma_y\sigma_z$. Anisotropy thus increases the second term in Eq. (7).

We finally consider emission (host fluorescence) for terminating the random walk by letting $\gamma \ll 1$ be finite. The existence of the limit $C_n(A)/n$ suffices to generalize Rudemo's¹⁸ formula for the emission probability in the special case $A=0$. The emission probability for a random walk with extended trapping regions is²⁶

$$Q(A, \gamma, n_T) = \frac{\gamma}{\gamma + n_T C(A)} \quad (8)$$

in the limit of small emission probability per step, or $\gamma \ll 1$, and long random walks on the average before absorption, or $n_T C(A) < n_T(A+1) \ll 1$. The ratio γ/n_T is arbitrary, however, and $Q(A, \gamma, n_T)$ is also a general result for three-dimensional random walks with finite extended trapping regions. The physical interpretation of $Q(A, \gamma, n_T)$ is straightforward: $Q(A, \gamma, n_T)$ describes the competition between host fluorescence with probability γ per step, and trapping with probability $n_T C(A)$ per step after many steps for terminating a very long random walk.

B. Capacities for Cubic Lattices

To illustrate the properties of extended trapping regions, we consider the familiar special case of a simple cubic lattice with one site per unit cell and nearest-neighbor steps with structure function

$$\lambda_0(x, y, z; \alpha) = \frac{1}{2+\alpha} (\cos x + \cos y + \alpha \cos z). \quad (9)$$

The subscript "0" will be reserved for quantities based on nearest-neighbor transition probabilities. The structure function λ_0 indicates that unit steps along the x or y axes have probabilities $[2(2+\alpha)]^{-1}$, while unit steps along the z axis occur with probability $\alpha[2(2+\alpha)]^{-1}$. Thus, $\alpha=1$ corresponds to isotropic random walk, while $\alpha>1$ represents preferential motion along the z axis and

reduces to a one-dimensional random walk in the limit $\alpha \rightarrow \infty$.

The Green's functions $G_0(\vec{a}; \alpha)$ for nearest-neighbor random walk are obtained by substituting λ_0 into Eq. (2) and using the fact that $\lambda(\vec{r})$ is real and symmetric for symmetric random walks

$$G_0(a, b, c; \alpha)$$

$$= \frac{(2+\alpha)}{\pi^3} \int_0^\pi \int_0^\pi \int_0^\pi \frac{\cos ax \cos by \cos cz \, dx \, dy \, dz}{(2+\alpha) - \cos x - \cos y - \alpha \cos z}. \quad (10)$$

Maradudin *et al.*²⁴ have tabulated the integrals

$$I(a, b, c; \alpha; \beta) = \frac{1}{\pi^3} \int_0^\pi \int_0^\pi \int_0^\pi \frac{\cos ax \cos by \cos cz \, dx \, dy \, dz}{(2+\alpha)\beta - \cos x - \cos y - \alpha \cos z} \quad (11)$$

for $a^2 + b^2 + c^2 < 15$, $\alpha = 1, 2, 4, 8, 16$, and $\beta^{-1} = \mu = 0.00$ (0.01)1.00. Direct comparison shows that

$$G_0(\vec{a}; \alpha) = (2+\alpha)I(\vec{a}; \alpha; 1). \quad (12)$$

For $\beta=1$ and $R^2 \gg 1$, the asymptotic formula²⁴

$$I(a, b, c; \alpha; 1) \sim \frac{1}{2\pi\sqrt{\alpha}R} + \frac{1}{16\pi\sqrt{\alpha}} \left(\frac{5(a^4 + b^4 + c^4/\alpha^3)}{R} - \frac{6(a^2 + b^2 + c^2/\alpha^2)}{R^5} + \frac{(2+1/\alpha)}{R^3} \right) + \dots \quad (13)$$

holds to order R^{-5} , as shown by Duffin²⁷ for $\alpha=1$. Here we define

$$R^2 = a^2 + b^2 + c^2/\alpha, \quad (14)$$

which reduces to $\vec{a} \cdot \vec{a}$ for $\alpha=1$. The Green's function for axially anisotropic nearest-neighbor transition probabilities are therefore known.

We begin by computing the capacities $C_0(A)$ for some representative trapping regions. The volume dependence of the trapping region is shown by considering $A=0, 6$, and 26 and spherical trapping regions; for $A=6$, the extended trapping region then includes the 6 nearest neighbors, while for $A=26$, the 26 neighbors less than two lattice spacings away are considered. The *shape* dependence of the extended trapping region is illustrated by $A=6$ and 26 , with $\frac{1}{2}A$ sites of the trapping region along the x or z axis on either side of the activator; a highly anisotropic, linear, symmetric trapping region is thus defined. Finally, the anisotropy of the random walk is illustrated by considering isotropic ($\alpha=1$) and anisotropic ($\alpha=8$) transition probabilities in λ_0 . In each case, we construct the $(A+1) \times (A+1)$ matrix of Green's functions $G(\vec{R}_i, \vec{R}_j)$, with i and j ranging over the extended trapping region, by either looking up $G_0(\vec{a}; \alpha) = (2+\alpha)I(\vec{a}; \alpha; 1)$ or using Eq. (13) for $a^2 \geq 15$. The matrices are then inverted numerically and the sum of the elements of the inverse matrix is the capacity $C_0(A)$. The results are given in Table I.

TABLE I. Capacities of extended trapping regions for nearest-neighbor random walk on a simple cubic lattice.

Extended trapping region		Random walk	
Volume $A + 1$	Shape	Isotropic ($\alpha = 1$)	Anisotropic ($\alpha = 8$)
1	point	0.659 463 ^{a, b}	0.459 329 ^a
7	spherical	1.936 52	1.337 10
	linear (\hat{x} or \hat{y})	2.263 01	1.749 46
	linear (\hat{z})	2.263 01	1.030 30
27	spherical	3.155 99	2.066 93
	linear (\hat{x} or \hat{y})	6.212 92	4.941 79
	linear (\hat{z})	6.212 92	2.452 06

^aReference 24; $C(0) = G^{-1}(0; 1)$.

^bReference 28.

Table I shows that $C_0(A)$ for nearest-neighbor walks varies markedly with the volume $A + 1$ of the extended trapping region as well as with the shape of the trapping region and the anisotropy of the random walk. The initial absorption probability for a freshly created exciton is $n_T(A + 1)$. The $n \rightarrow \infty$ asymptotic absorption probability $n_T C_0(A)$ is obtained by substituting Eq. (7) into Eq. (4). The ratio $C_0(A)/(A + 1)$ thus describes the asymptotic to initial trapping probability per step. The rapid decrease of $C_0(A)/(A + 1)$ with increasing A is illustrated in Table I by the isotropic ($\alpha = 1$) walk and spherical extended trapping regions: $C_0(0) = 0.660$, the well-known result^{21, 22, 28} for trapping on the first visit to a trapping site; $C_0(6)/7 = 0.277$ and $C_0(26)/27 = 0.117$. Physically, extended trapping regions permit the random walker to sample more sites initially, but greatly increasing the resampling for nearest-neighbor steps. Resampled sites cannot be activators, since the walk would then have been previously terminated and thus cannot lead to trapping as already shown in Eq. (4). The decrease of $C_0(A)/(A + 1)$ with increasing anisotropy α of the random walk is also expected, since the limits $\alpha \rightarrow 0$ or $\alpha \rightarrow \infty$ lead to symmetric random walks in two and one dimensions, respectively, and such walks are recurrent with $C(0) \rightarrow 0$. It should be noted that significant changes in $C_0(A)$ are possible, as shown in Table I, for less than an order of magnitude of axial anisotropy ($\alpha = 8$), especially when the trapping region is also anisotropic.

C. LRRT Distribution of Steps

Only nearest-neighbor transitions are included in $\lambda_0(\vec{r})$ in Eq. (9). Longer steps, especially those that exceed the dimensions of the extended trapping region, strongly influence the rate of sampling sites for the first time. Consider, for example, only steps of three lattice spacings along the $x, y,$

and z axes. The random walker is then confined to a superlattice with 27 points of the original lattice per site. If the spherical extended trapping region consisting of the 26 neighbors less than two lattice spacings away is chosen, then the walker samples either all 27 sites for the first time or resamples them all. The ratio $C(26)/27$ reduces to 0.660; the simple cubic result for the superlattice. Steps of length three thus reduce the resampling by $0.660/0.117 \sim 6$. Indeed, if we consider steps with probability N^{-1} to all lattice points, the $N \rightarrow \infty$ limit leads to $G(0) \rightarrow 1$ and $G(\vec{a}) \rightarrow 0$ for $\vec{a} \neq 0$. The exciton never returns to a previously sampled site and $C_\infty(A) = A + 1$. Long steps thus increase $C(A)$, but also increase σ^2 in Eq. (6) and thus do not necessarily increase the coefficient of the $n^{-1/2}$ term in Eq. (7) describing the approach of $C_n(A)$ to $C(A)$.

The LRRT^{3, 4} model for energy transfer leads to a rate dependence of r^{-6} for steps of length r . We suppress the angular dependence of the transition probabilities and adopt an isotropic ($\alpha = 1$) distribution of step lengths $P(\vec{a}) = P(|a|) = (6\beta\alpha^6)^{-1}$. The constant β is given by

$$\beta = 1 + \frac{1}{6} \sum_{\vec{a}} \alpha^{-6}, \quad |a| > 1 \quad (15)$$

where the sum is over the points of a simple cubic lattice. The structure function $\lambda(\vec{r})$ in Eq. (3) then becomes

$$\lambda(\vec{r}) = \beta^{-1} [\lambda_0(\vec{r}) + \lambda_1(\vec{r})], \quad (16)$$

where $\lambda_0(\vec{r})$ is the nearest-neighbor function in Eq. (9) and $\lambda_1(\vec{r})$ is

$$\lambda_1(\vec{r}) = \frac{1}{6} \sum_{\vec{a}} \alpha^{-6} e^{i\vec{r} \cdot \vec{a}}, \quad |a| > 1. \quad (17)$$

The exciton-diffusion constant²⁹ D for an isotropic random walk with an average time τ between steps is given by

$$D = \frac{1}{2} \sigma^2 \tau^{-1}, \quad (18)$$

where σ^2 is defined in Eq. (6) and, for an LRRT distribution of step lengths, is

$$\sigma^2 = (1/18\beta) \sum_{\vec{a}} \alpha^{-4}. \quad (19)$$

The totally isotropic random walk adopted here provides a mathematically convenient, but still oversimplified, model for investigating the effects of steps longer than one lattice spacing.

By truncating Eqs. (15) and (17) at $|a| = p$, we obtain β_p and $\lambda_1^{(p)}(\vec{r})$ for an LRRT distribution of steps up to length p and no steps longer than p . The $p = 1$ result reduces to nearest-neighbor steps only, and as required to $\beta_1 = 1$. The Green's function for LRRT steps up to length p are

$$G^{(p)}(\vec{a}) = \frac{3\beta_p}{\pi^3} \int_0^\pi \int_0^\pi \int_0^\pi \frac{\cos ax \cos by \cos cz \, dx \, dy \, dz}{\beta_p - 3\lambda_0(\vec{r}) - 3\lambda_1^{(p)}(\vec{r})}. \quad (20)$$

TABLE II. Capacities for LRRT distribution of step lengths for isotropic random walk on a simple cubic lattice.

p^a	β_p^b	$3\sigma_p^2^c$	$C(0)=G^{-1}(0)$	$C(26)^d$
1 ^e	1.000 0000	1.000 000	0.659 462	3.155 99
$\sqrt{6}$	1.365 5264	1.451 285	0.763 11	4.380 8
$\sqrt{14}$	1.388 8042	1.599 606	0.784 62	4.962 7
$\sqrt{27}$	1.395 5911	1.690 426	0.791 12	5.160 5
$\sqrt{29}^f$	1.400 3000	1.782 26	0.795 46	5.296 8

^aLength of longest step (in lattice spacings).

^bSee Eq. (15).

^cSecond moment; see Eqs. (6) and (19).

^dSpherical extended trapping region of 27 points.

^eNearest-neighbor steps only.

^fThe probabilities for all steps longer than $\sqrt{27}$ are lumped into the (2, 3, 4) step.

It is important to preserve the normalization condition $\lambda_0(0) + \lambda_1^{(p)}(0) = 1$ for whatever p is chosen, since $G^{(p)}(\vec{a})$ has an integrable singularity at the origin. $G^{(p)}(\vec{a})$ can readily be evaluated numerically by Gauss-Legendre integration.³⁰ To check convergence, especially in view of the singularity at the origin, the ten Green's functions $G_0(\vec{a})$ with $0 \leq a, b, c \leq 2$ and $\alpha = 1$ were evaluated using (28)³ and (64)³ points in the triple integral. The former agreed to four significant figures when compared against the previous numerical results²⁴ for a nearest-neighbor random walk; the latter were accurate to almost five significant figures. The more rapid (28)³ point integration was used throughout, with occasional checks using (64)³ points, and the numerical results below are accurate to ± 0.0005 .

In Table II we list values for $C(0) = G^{-1}(0)$, $C(A)$ for a spherical trapping region of 27 points, and σ^2 for isotropic LRRT steps up to $p = \sqrt{6}$, $\sqrt{14}$, and $\sqrt{27}$, respectively. In addition, we estimate $\beta = 1.4003$ by integrating Eq. (15) for $|a| \geq \sqrt{28}$ and using the computed value of the sum for $1 < |a| \leq \sqrt{27}$. All steps longer than $\sqrt{27}$ were lumped into the steps (2, 3, 4) of length $\sqrt{29}$. As can be seen in Table II, $C(A)$ increases by about a factor of 2 when the spherical trapping region of 27 points is used. By contrast, the change in $C(0) = G^{-1}(0)$ is small. For an anisotropic random walk, when $C_0(0)$ is much less than the isotropic value of 0.660, long steps can provide a greater increase. Of course the restriction²¹ $C(A) \leq A + 1$ holds for any random walk and provides an upper bound for $C(A)$.

Tables I and II thus show that the capacity $C(A)$ depends on the shape and size of the extended trapping region, on the anisotropy of the random walk, and on the distribution of step lengths. The

combination of a large, anisotropic trapping region and an anisotropic random walk with an LRRT distribution of step lengths can easily produce more than an order of magnitude change between $C(A)$ and $C(0) = G^{-1}(0)$, the result for trapping on the first visit to an activator site.

We have therefore shown that the capacity $C(A)$ can readily be computed for arbitrary finite trapping regions and that the Green's functions $G(\vec{a})$ for a simple cubic lattice can also be computed even for an LRRT distribution of step lengths. It should be mentioned that the generalization of Rudemo's¹⁸ result for the host fluorescence to extended trapping regions $Q(A, \gamma, n_T)$ in Eq. (8) is the only rigorous result for a general transient random walk with *both* emission and absorption. The approach of $C_n(A)$ to $C(A)$ given Eq. (7) is derived for an isotropic random walk in the absence of emission. The analysis of extended trapping regions and of emission for a random walker on a simple cubic lattice will now be used to discuss qualitatively the PK results in doped anthracene and naphthalene crystals.

III. ANTHRACENE AND NAPHTHALENE

The small activator density n_T and even smaller singlet exciton density used in the PK experiment⁶⁻¹¹ permit neglecting exciton-exciton interactions and trap saturation. The average behavior of a singlet exciton is given by the random variable $C_n(A)$ for sampling lattice points for the first time. The probability for trapping on the n th step, p_n in Eq. (4), is readily transformed to a rate of energy transfer $k(t)$ by introducing a mean time τ between steps. Then $t = n\tau$ and from Eq. (7),

$$k(t) = n_T C(A) \tau^{-1} \left[1 + \frac{2C(A)}{(2\pi\sigma^2)^{3/2}} \left(\frac{\tau}{t} \right)^{1/2} + \dots \right] \quad (21)$$

for $t \gg \tau$ (i. e., for $n \gg 1$), with corrections of order t^{-1} . The asymptotic form of $k(t)$ does not depend on the transition probabilities defining the three-dimensional host lattice; it does not depend on the distribution of step lengths and it does not depend on the volume or shape of the extended trapping region. The assumption of constant time intervals τ between steps is justified²² after many steps. The detailed nature of the transition probabilities of the lattice geometry and of the extended trapping region enter through the parameters $C(A)$ and σ^2 whose evaluation was discussed in Sec. II for a simple cubic lattice. The rate of energy transfer $k(t)$ is now obtained numerically¹⁶ from PK data.⁶⁻¹¹ An understanding of the time dependence of $k(t)$ is the principal challenge of the time-resolved fluorescence spectroscopy results.

The dependence of the sensitizer emission probability $Q(A, \gamma, n_T)$ in Eq. (8) on the activator concentration n_T provides another comparison with ex-

periment. $Q(A, \gamma, n_T)$ is a direct measure of the quenching of the total sensitizer (host) fluorescence $I_s(n_T)$ with increasing n_T . Rearranging Eq. (8), we obtain

$$I_s(0)/I_s(n_T) = Q^{-1}(A, \gamma, n_T) = 1 + n_T C(A)/\gamma \quad (22)$$

provided that the restrictions $\gamma \ll 1$ and $n_T C(A) < n_T(A+1) \ll 1$ are satisfied. Fluorescence-quenching experiments^{19,20} thus provide estimates for $C(A)\gamma^{-1}$. No assumptions about anisotropies or lengths of steps or about the extended trapping region are required in Eq. (22) unless a numerical estimate of $C(A)$ is attempted. $I_s(0)/I_s(n_T)$ data provide an estimate of $C(A)\tau^{-1}$, since the emission probability per step γ is simply

$$\gamma = \beta_s \tau \quad (23)$$

and the undoped-sensitizer-fluorescence decay rate β_s is readily measured. The asymptotic rate of energy transfer

$$k(\infty) = n_T C(A)\tau^{-1} \quad (24)$$

also provides an estimate for $C(A)\tau^{-1}$.

The numerical results in Sec. II were obtained for a simple cubic lattice and the second term in Eq. (21) is based on an isotropic random walk in the absence of emission. We therefore do not attempt a quantitative fit of $k(t)$, $k(\infty)$, and $I_s(0)/I_s(n_T)$ data for doped anthracene and naphthalene crystals. Rather, we note that the $t^{-1/2}$ term in Eq. (21) contributes up to times $[C(A)/C(0)]^2$ longer for an extended trapping region and a fixed random walk (fixed σ^2). The variations in $C(A)$ with the volume and shape of the extended trapping region and with the anisotropy and step distribution of the random walk thus indicate that the second term in Eq. (21) is important up to times several orders of magnitude longer than expected when trapping occurs on the first visit to an activator site. And it is just the rapid convergence of $k(t)$ to $k(\infty)$ that spoils⁶⁻¹¹ the usual formulation of exciton trapping and either nearest-neighbor random walking or diffusion. Experimental evidence over some two orders of magnitude variations in $C(A)$ for different activators in naphthalene then provides strong qualitative support for extended trapping regions.

A. Time Dependence of $k(t)$

The rate of energy transfer $k(t)$ of singlet excitations from the sensitizer to the activator is obtained from the time dependence of the host and trap fluorescence studied by PK⁶⁻¹¹ in doped organic crystals and described by the kinetic equations

$$\begin{aligned} \dot{n}_S(t) &= G(t) - \beta_S n_S(t) - \int_{-\infty}^t G(t') k(t-t') n_{S_i}(t-t') dt', \\ \dot{n}_A(t) &= \int_{-\infty}^t G(t') k(t-t') n_{S_i}(t-t') dt' - \beta_A n_A(t). \end{aligned} \quad (25)$$

n_S and n_A are, respectively, the sensitizer (host exciton) and the excited activator (guest or trap) concentrations; $G(t)$ is the exciton generating function, which in the PK experiments is either an x ray or a laser pulse and leads to negligible activator excitation; β_S and β_A are the measured inverse-fluorescence lifetimes of the sensitizer (host) and activator (trap). The solution for $n_S(t)$ in Eq. (25) is a convolution of the excitation function with the response function for singlet excitons

$$n_{S_i}(t) = \int_{-\infty}^t G(t') n_{S_i}(t-t') dt',$$

where

$$n_{S_i}(t-t') = \exp[-\beta_S(t-t') - \int_{t'}^t k(t''-t') dt''] . \quad (26)$$

The variation of $n_S(t)$ and $n_A(t)$ are directly reflected by the time evolution of the host and trap fluorescence $I_s(t)$ and $I_A(t)$ reported by PK⁶⁻¹¹ and analyzed by them for various functional choices of $k(t)$.

Numerical values for the time evolution of $k(t)$ in Eqs. (25) and (26) are obtained as follows.¹⁶ First, smooth curves are drawn through the PK-fluorescence curves. Here it is important to note that these data are normalized to unity at the maximum observed fluorescence and thus will yield relative rather than absolute $k(t)$ values. Next, we consider time intervals of ϵ and assume that $k(t)$, the most slowly varying quantity in Eqs. (25) and (26), is constant during each interval. For a δ -function excitation pulse, the second equation in (25) can be integrated to give³¹

$$k((p + \frac{1}{2})\epsilon) \approx \frac{e^{\beta_A(p+1)\epsilon} n_A((p+1)\epsilon) - n_A(p\epsilon) e^{\beta_A p\epsilon}}{\int_{p\epsilon}^{(p+1)\epsilon} e^{\beta_A t'} n_{S_i}(t') dt'} \quad (27a)$$

for $p=0, 1, 2, \dots$ and $n_A(0)=0$ if direct trap excitation is neglected. Equation (27a) then yields experimental $k(t)$ values, since all quantities on the right are measured. Finally, the relative $k(t)$ values for a given activator concentration in a given sensitizer are normalized to give the best superposition for the time dependences.

The δ -function excitation is in an excellent approximation for the laser pulse and is actually not too bad for the x-ray pulse with a 2.5-nsec full width at half-maximum.³¹ However, for the latter case, a somewhat different procedure is more accurate at short times. $G(t)$ for the x-ray pulse will be nonzero for about the first 5 nsec. Thus, from Eqs. (25) and (26),

$$n_{S_i}(t) = \int_0^5 G(t') n_{S_i}(t-t') dt',$$

$$\dot{n}_A(t) + \beta_A n_A(t) = \int_0^5 G(t') n_{S_i}(t-t') k(t-t') dt'.$$

Now if we consider 5-nsec intervals and treat $k(t)$ as a constant within each interval, we find

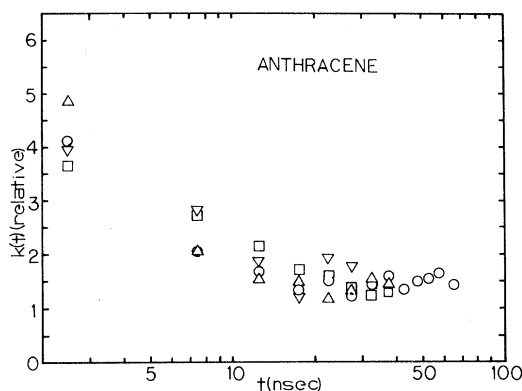


FIG. 1. Time dependence of the energy-transfer rate in tetracene-doped anthracene under the following conditions: O, thick crystal with 4.7×10^{15} -cm $^{-3}$ tetracene and x-ray excitation at $\sim 300^\circ\text{K}$; Δ , the same crystal excited by two-photon absorption at $\sim 300^\circ\text{K}$; ∇ , a thin crystal with 4.7×10^{15} -cm $^{-3}$ tetracene excited by x rays at 100°K ; and \square , the same thin crystal x ray excited at $\sim 300^\circ\text{K}$.

$$k(t - 2.5) \approx [\dot{n}_A(t) + \beta_A n_A(t)] / n_S(t). \quad (27b)$$

The curves for the activator fluorescence can be numerically differentiated so all of the quantities on the right side of Eq. (27b) can be measured.

Relative curves for $k(t)$ obtained as described above using Eq. (27a) for laser excitation (with $\epsilon = 5$) and Eq. (27b) for x-ray excitation are shown in Fig. 1 for tetracene-doped anthracene and in Fig. 2 for anthracene- or tetracene-doped naphthalene. Although the n_T dependence of $k(t)$ is lost by using this procedure, we show below that absolute $k(\infty)$ values can be obtained for samples with different n_T by focusing on the host fluorescence.

The data in Figs. 1 and 2 represent a variety of experimental conditions. The tetracene-doped anthracene results in Fig. 1 represent^{8,9}: (i) a thick crystal with 4.7×10^{15} -cm $^{-3}$ (~ 1 ppm) tetracene and x-ray excitation at $\sim 300^\circ\text{K}$; (ii) the same crystal excited by two-photon absorption at 300°K ; (iii) a thin crystal with 4.7×10^{15} -cm $^{-3}$ tetracene excited by x rays at 100°K ; and (iv) the same thin crystal x ray excited at $\sim 300^\circ\text{K}$. The naphthalene data shown in Fig. 2 were all obtained with x-ray excitation and represent^{9,11}: (i) a thick crystal with 3.9×10^{15} -cm $^{-3}$ (~ 0.7 ppm) anthracene; (ii) a thin crystal with 4.7×10^{17} -cm $^{-3}$ (~ 87 ppm) anthracene; (iii) a thick crystal with 3.3×10^{17} -cm $^{-1}$ (~ 61 ppm) anthracene; and (iv) a thin crystal with 1.4×10^{17} -cm $^{-3}$ (~ 26 ppm) tetracene. As shown elsewhere,¹⁶ the wide variety of experimental parameters investigated by PK⁶⁻¹¹ in an effort to understand the time dependence of $k(t)$ provides stringent conditions on adjustable parameters in theoretical models.

The failure of the usual formulation of exciton

diffusion⁶⁻¹¹ which leads to a constant $k(t)$ except at short times of no interest on the nanosecond time scale, is clearly shown by the time dependence of $k(t)$ shown in Figs. 1 and 2. The considerable scatter of the data does not obscure the fact that $k(t)$ decreases in both doped-anthracene and -naphthalene crystals. An asymptotic value, which we will associate with $k(\infty)$ in Eq. (24), is approached after 30 nsec in anthracene and, less certainly, after 60 nsec in naphthalene.

The absolute value of $k(\infty)$ can be estimated from the sensitizer (host) fluorescence. Integrating Eq. (25) gives

$$I_S(t) \propto n_S(t) = \exp(-\beta_S t + \int_0^t k(t') dt') \quad (28)$$

for $G(t) \propto \delta(t)$ and $n_S(0) = 1$. The host fluorescence thus decays exponentially for large t , when $k(t) \sim k(\infty)$, even if $k(t)$ is not constant at small t . The exponential long-time decay for the host fluorescence of two anthracene crystals (1- and 83-ppm tetracene) and of two naphthalene crystals (1- and 61-ppm anthracene) are shown in Fig. 3. $k(\infty)$ is found from the difference in the slopes of the doped and undoped samples, also shown in Fig. 3, at long time. The lightly doped naphthalene (1-ppm) crystal decays only slightly faster ($< 0.1 \times 10^7 \text{ sec}^{-1}$) than the undoped crystal and does not provide an accurate $k(\infty)$, while the heavily doped (83-ppm) anthracene decays too rapidly to provide an accurate $k(\infty)$. In both cases, however, the data are consistent with $k(\infty)$ proportional to n_T . The measured value of $k(\infty)$ for anthracene is $0.3 \times 10^7 \text{ sec}^{-1}$ for $n_T = 10^{-6}$ and $\beta_S = 3.7 \times 10^7 \text{ sec}^{-1}$; the measured undoped decay rate; the value of $k(\infty)$ for naphthalene is $1.5 \times 10^7 \text{ sec}^{-1}$ for $n_T = 61 \times 10^{-6}$ and $\beta_S = 0.94 \times 10^7 \text{ sec}^{-1}$, the measured undoped decay rate.

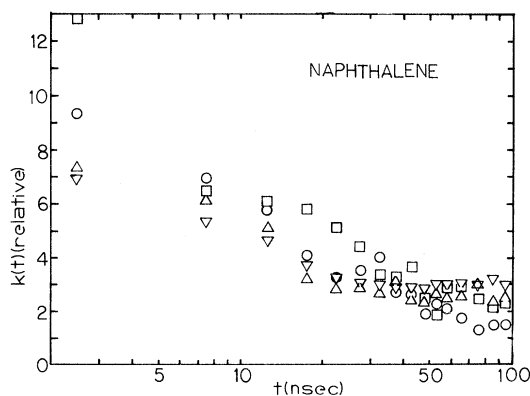


FIG. 2. Time dependence of the energy-transfer rate in x-ray excited naphthalene crystals at room temperature under the following conditions: Δ , thick crystal with 3.9×10^{15} -cm $^{-3}$ anthracene; O, thin crystal with 4.7×10^{17} -cm $^{-3}$ anthracene; ∇ , thick crystal with 3.3×10^{17} -cm $^{-1}$ anthracene; and \square , thin crystal with 1.4×10^{17} -cm $^{-3}$ tetracene.

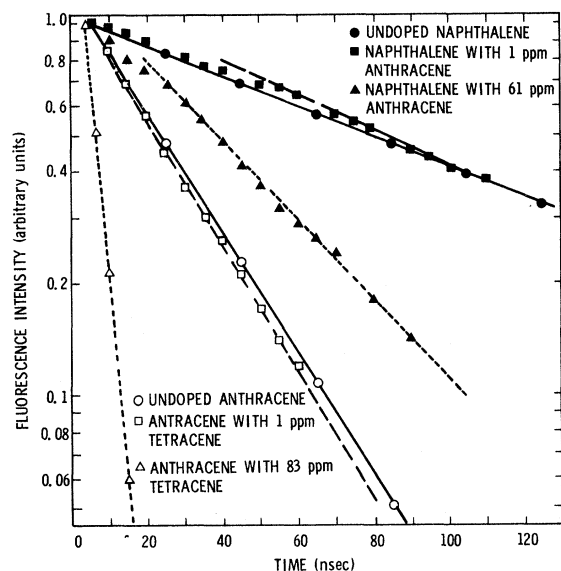


FIG. 3. Semilog plot of the long-time host fluorescence for doped anthracene (\circ , undoped; \square , 1-ppm tetracene; \triangle , 83-ppm tetracene) and for doped naphthalene (\bullet , undoped; \blacksquare , 1-ppm anthracene; \blacktriangle , 61-ppm anthracene).

B. Evidence for Extended Trapping Regions

A popular method¹⁹ for investigating energy transfer in doped organic crystals has been to monitor the quenching of the sensitizer-(host) fluorescence intensity or decay time as a function of activator concentration n_T . The data are interpreted in terms of

$$I_s(0)/I_s(n_T) = 1 + \kappa n_T, \quad (29)$$

where $I_s(n_T)$ and $I_s(0)$ are, respectively, the host-fluorescence intensities for doped and undoped samples. If I_s decays exponentially, then the ratio $\beta_s(n_T)/\beta_s(0)$ of the host-fluorescence decay rates can be used in Eq. (29). The proportionality constant κ is obtained from the slope of $I_s(0)/I_s(n_T)$ vs n_T curves and is to be related to theoretical models. In the "hopping model" generally used to describe exciton motion,¹⁹ κ is given by

$$\kappa = (\beta_s \tau_{app})^{-1}, \quad (30)$$

where τ_{app} is the apparent mean time between exciton jumps in the host lattice. It has implicitly been assumed in obtaining τ_{app} that trapping occurs on the first visit to a trapping site, or that $C(A) \sim 1$ in Eq. (22).

A curious consequence of this type of analysis has been that different apparent hopping times have been reported for different activators in the same host.^{19,20} For example, the apparent hopping times for naphthalene doped with various activators range from 3.2×10^{-14} to 8.5×10^{-12} sec, as

shown in Table III. The hopping time is of course an intrinsic property of the host. The variation of the apparent hopping time based on Eq. (30) for κ is thus an important, and previously overlooked, indication that the model of trapping on the first visit to an activator site is inadequate.

The generalization of Rudemo's result for the emission probability to extended trapping regions provides a microscopic theory for κ and, as shown in Eq. (22), leads to $\kappa = C(A)/(\beta_s \tau)$. The extended trapping region, whose properties depend on the shape of the activator and on the depths of the trap thus enters naturally and Table III provides strong evidence for significant variations of $C(A)$ with different activators in naphthalene. Even if the trap concentration n_T is too large to permit the asymptotic form $Q(A, \gamma, n_T)$ in Eq. (8), an approximately linear relation of $Q^{-1}(A, \gamma, n_T)$ vs n_T is expected, with the coefficient slightly larger than $C(A)$. A detailed analysis of the experimental uncertainties in fluorescence-quenching data may thus provide experimental estimates of $C(A)$ for various activators.

There are thus two results for $k(\infty) = C(A)\tau^{-1}$ for anthracene-doped naphthalene. The PK value¹¹ based on $k(\infty) = 1.5 \times 10^7 \text{ sec}^{-1}$ for $n_T = 61 \times 10^{-6}$ discussed above leads to $C(A)\tau^{-1} = 2.5 \times 10^{11} \text{ sec}^{-1}$. The inverse of the apparent hopping time¹⁹ of $4 \times 10^{-12} \text{ sec}^{-1}$ in Table III also leads to $C(A)\tau^{-1} = 2.5 \times 10^{11} \text{ sec}^{-1}$. Such agreement has been used⁶⁻¹¹ to demonstrate that time-resolved fluorescence spectroscopy data are consistent with previous studies in which the time evolution of $k(t)$ was not measured.

It is tempting to assign the *smallest* apparent hopping time in Table III to be the result for trapping on the first visit to an activator site. Even then, however, Eq. (30) could not be used to obtain τ . The reason is that $C(0) = G^{-1}(0)$ may be substantially less than unity for an anisotropic random walk, as shown in Table I. It is therefore not possible to extract a purely experimental value for τ from $I_s(0)/I_s(n_T)$ data.

Craig and his co-workers^{32,33} were led to postulate extended trapping regions to account for the efficient transfer of energy from host to activator

TABLE III. Apparent singlet-exciton hopping times in naphthalene crystals doped with different activators.

Activator	$\tau_{app}(\text{sec})^a$	Reference
β methylnaphthalene	10^{-13}	20(a)
Anthranilic acid	1.5×10^{-13}	20(c); also quoted in 20(b)
1,4 diphenylbutadiene	3.2×10^{-14}	20(c); also quoted in 20(b)
1,6 diphenylbutadiene	4.0×10^{-13}	20(c); also quoted in 20(b)
Anthracene	4.0×10^{-12}	19; also from data in 20(d)
Acridine	4.2×10^{-12}	From data in 20(d)
Tetracene	8.5×10^{-12}	From data in 11

^aSee Eq. (30).

even when, as in tetracene-doped naphthalene, the activator- and sensitizer-energy difference is large. The successive emission of several phonons upon trapping occurs with too low probability to account for the efficient observed energy transfer. The suggestion^{32,33} is that in mixed crystals the host-exciton energy bands bend to lower energy in the vicinity of a deep-trap (activator) molecule. A smaller amount of energy must then be dissipated thermally upon trapping and trapping occurs more efficiently. No estimates of the trapping region were proposed, although the neutral activator is not expected to change the electronic levels of sensitizers more than a few lattice spacings away. Extended trapping regions thus arise naturally in several contexts, but have not been susceptible to direct measurement. The variation of $C(A)$ with different activators in the same host may thus provide the most direct method for studying the trapping mechanism.

IV. DISCUSSION

The random-walk model for exciton trapping developed in Sec. II is a natural generalization of the diffusion result^{8,29,34} for absorption by a sphere of radius R_0 ;

$$k_D(t) = 4\pi DR_0 n_T [1 + R_0/(\pi Dt)^{1/2}]. \quad (31)$$

Here $D = \frac{1}{2}\sigma^2\tau^{-1}$ is the exciton-diffusion constant. The time dependence of $k_D(t)$ and of the random-walk result $k(t)$ in Eq. (21), are identical asymptotically. Even the volume dependence of the trapping region is the same, since the capacity $C(A)$ is proportional²¹ to the radius of the trapping region and occurs in $k(t)$ in the same manner that R_0 occurs in $k_D(t)$.

There are several important advantages to the microscopic random-walk model. The extended trapping region arises naturally, while the interpretation of R_0 in $k_D(t)$ is difficult.¹⁹ Even more important is that anisotropic extended trapping regions can readily be included and that the effects of different step lengths, which are completely obscured in the diffusion limit, pose no difficulties. It is evident that a scalar parameter like R_0 can at best reproduce the volume dependence of $C(A)$. The dependence of $C(A)$ on the shape of the trapping region, on the anisotropy of the random walk, and on the distribution of step lengths is summarized in Tables I and II and must be considered in any but the most qualitative model.

The inadequacy of $k_D(t)$ is perhaps best shown by considering the radius R_0 required to fit the $k(t)$ data in Figs. 1 and 2. The estimate of $R_0 \sim 5-10$ Å for trapping on the first visit to an activator leads⁸ to $t \lesssim 10^{-11}$ sec before the constant term in Eq. (31) dominates. The PK data in Figs. 1 and 2 require R_0 values of at least 100 Å, with $R_0 \sim 130$

Å providing a reasonable fit for doped anthracene. Taking a typical lattice spacing of 8 Å, we see that an extended trapping region of 10-20 neighbors is required, and such an enormous trapping region is not physically reasonable for a neutral substitutional impurity.

The generalized random-walk model, on the other hand, requires far smaller extended trapping regions to fit the PK data. Although the quantitative results in Sec. II for a simple cubic lattice cannot be applied directly to singlet-exciton motion in monoclinic anthracene or naphthalene crystals, it is nevertheless interesting to consider the qualitative picture for exciton trapping which emerges from an analysis of the time-resolved spectroscopy data in terms of Eq. (21) for $k(t)$.

The generalized random-walk model requires three parameters besides the (known) activator concentration n_T : (i) the capacity $C(A)$ for the extended trapping region adopted for a particular activator; (ii) the mean time τ between jumps; (iii) the mean-square length of the steps $3\sigma^2$ in units of the lattice constant. As shown in Eq. (18), the exciton-diffusion constant D can be used to eliminate σ^2 . An immediate consequence of the model is that the host lattice enters in τ and σ^2 (and thus in D), while the activator is described by the extended trapping region. Different activators in the same sensitizer should only require different $C(A)$ values.

Two estimates for $C(A)$ and τ are obtained if we choose $\frac{1}{2} \leq 2\sigma^2 \leq 1$, which is consistent with the σ^2 values in Table II. First, specific $I_s(t)$ and $I_A(t)$ curves, for example those in Figs. 1-4 of Ref. 8, give excellent fits when Eqs. (25) and (26) are solved using a combined³⁵ theory, with exciton diffusion and LRRT to the traps, for $k(t)$. The combined theories, which fail only because they require anomalous parameters,^{8,11} lead to $k(t) \propto t^{-1/2}$ at short t and to constant $k(t)$ asymptotically. The generalized random-walk model, which is based on extended trapping regions and a distribution of host-host steps, leads to $k(t)$ in Eq. (21) and gives the same excellent fits, but with quite different interpretation of the parameters. For $\frac{1}{2} < 2\sigma^2 < 1$, the results are $C(A) \sim 19-38$ and $\tau \sim (1-3) \times 10^{-10}$ sec for doped naphthalene; the corresponding values for doped anthracene are $C(A) \sim 35-70$ and $\tau \sim (3-6) \times 10^{-11}$ sec. The smaller $C(A)$ and τ values hold for $2\sigma^2 = \frac{1}{2}$, which may be more appropriate since anisotropy reduces σ^2 . The $\tau/C(A)$ values are in excellent agreement with Wolf's apparent hopping times¹⁹: 3×10^{-13} sec for anthracene: tetracene and 4×10^{-12} sec for naphthalene: anthracene.

Another estimate for $C(A)$ and τ , this time for all the samples shown in Figs. 1 and 2, is obtained by again choosing $\frac{1}{2} \leq 2\sigma^2 \leq 1$ and using Fig.

3 to obtain $C(A)\tau^{-1}$ experimentally. The coefficient of the $t^{-1/2}$ term in Eq. (21) then provides another relation between $C(A)$ and τ . In spite of the considerable scatter, either Fig. 1 for doped anthracene or Fig. 2 for doped naphthalene give reasonably straight lines when plotted against $t^{-1/2}$; the slope is the desired coefficient. The results for naphthalene are $C(A) \sim 6-60$ and $\tau \sim 4-40 \times 10^{-11}$ sec; for anthracene $C(A) \sim 30-80$ and $\tau \sim 1-6 \times 10^{-11}$ sec. Again, the smaller values of $C(A)$ and τ correspond to $2\sigma^2 = \frac{1}{2}$. The greater uncertainties reflect the greater number of experiments being fitted.

As shown in Tables I and II, either an anisotropic trapping region or an LRRT step distribution can double the capacity. Thus, even for an extended trapping region of 27 lattice points, or of only two neighbors, $C(A)$ values of 7-10 are possible when the trapping region is anisotropic and steps longer than nearest neighbor are included. The proportionality²¹ of $C(A)$ to the radius for a large spherical trapping region is very well satisfied even for the radii of 0, 1, and 2 given in Table I. Extended trapping regions of around 5 neighbors are thus sufficient in either naphthalene or anthracene. As emphasized already, these estimates are qualitative, since Eq. (21) was derived for an isotropic random walk and the numerical results are for a simple cubic lattice. The values of the capacity estimated above seem somewhat large for a neutral impurity and would require the host molecules within about five lattice spacings are perturbed by the presence of each activator. However, it is easy to see that the generalized random-walk model leads to substantially smaller estimates than the 10-20 lattice-spacing radius obtained from $k_D(t)$, since both the anisotropy of the trapping region and the step distribution increase $C(A)$ without increasing the trapping volume $A+1$.

We have concentrated on demonstrating that the generalized random-walk model for exciton migration is consistent with the time dependence of the energy-transfer rate and with the variation of the apparent hopping times for different activators in the same host. These are the two observations which cannot be explained by the usual formulation of exciton diffusion theory. The generalized random-walk model is also consistent with other observations which are satisfactorily predicted by exciton-diffusion theory. The model does not, for example, alter the interpretation of Simpson's⁵ experiment demonstrating singlet exciton diffusion in anthracene. In contrast with the PK experiment of randomly distributed, isolated microscopic traps, Simpson used a macroscopic ($\sim 1-\mu$) layer of heavily tetracene-doped anthracene as a detector behind an equally thin layer of pure anthracene. Singlet excitons created in the anthracene layer are trapped and detected as tetracene fluorescence

if they cross the interface with the heavily doped region. Since the diffusion length of 460 Å is many times 5-10-Å lattice spacing, the diffusion limit is appropriate. Neither an extended trapping region of a few lattice spacings nor an LRRT distribution of host-host steps is then important. The former merely shifts slightly the (poorly defined) interface between doped and undoped regions; the latter contributes to the diffusion constant whose magnitude is to be determined from the experiment. A more thorough, microscopic analysis of the random walk and of the trapping mechanism is only required in the more complicated, and potentially more interesting, situation of microscopic trapping regions.

There is considerable evidence^{19,20} showing that the quenching of the host-fluorescence intensity and decay time varies linearly with activator concentration. At the long times where those measurements are made, the generalized random-walk model predicts a constant-energy-transfer rate, $k(\infty)$ in Eq. (24), proportional to activator concentration and is therefore consistent with results of this type.

The results of temperature-dependence studies are generally too complicated to be currently useful in characterizing energy transfer.¹⁶ The host-fluorescence lifetime changes with temperature due to changes in reabsorption or exciton trapping; the exciton motion is sensitive to changes in thermal or defect scattering or to trapping by host traps, and both the hopping rate and trapping rate may change due to spectral overlap changes. These changes should have similar effects on both exciton-diffusion and generalized random-walk models, and neither of these theories is inconsistent with the experimental results which have been reported.⁹ It should be mentioned, however, that at low temperatures¹⁷ in pure crystals the exciton may move coherently instead of incoherently and neither the generalized random-walk nor the exciton-diffusion models may then be appropriate. Studies of temperature and sample-size effects indicate⁹ that radiative reabsorption is greatly decreased for small samples and at low temperatures. Experimentally, it has been shown that radiative reabsorption has only a small effect on the time resolved-spectroscopy results (except for an over-all lifetime lengthening effect) and exciton-diffusion theory still is not satisfactory even when reabsorption is minimized. Although host reabsorption acts as a long step in the exciton random walk, these steps take place at a very slow rate (approximately the host-fluorescence decay rate) and are too slow to alter the time development of $k(t)$.

In summary, the present model generalizes the usual diffusion model for exciton trapping by postulating an extended trapping region and by treating

explicitly steps of arbitrary length. The generalized random-walk model reconciles, at least qualitatively, the time dependence of $k(t)$ observed by PK⁶⁻¹¹ with singlet-exciton diffusion at room temperature in organic solids. Extended trapping regions provide a straightforward interpretation for the different apparent hopping times reported^{19,20} for naphthalene doped with different activators. The properties of extended trapping regions and of an r^{-6} step distribution were obtained for random walks on a simple cubic lattice, but can readily

be generalized to any lattice whose Green's functions are known.

ACKNOWLEDGMENTS

We would like to thank R. G. Kepler, L. A. Harrah, and R. C. Hughes for valuable discussions and criticisms, and one of us (Z. G. S.) would like to thank them for their hospitality during a sabbatical at Sandia Laboratories. We also thank A. J. Silverstein for his assistance with the computations.

*Work supported by U. S. Atomic Energy Commission.

†Alfred P. Sloan Fellow, 1969-71. Permanent address: Department of Chemistry, Princeton University, Princeton, N. J. 08540.

‡Present address: Department of Physics, Oklahoma State University, Stillwater, Okla. 74074.

¹J. Frenkel, *Physik. Z. Sowjetunion* **9**, 158 (1936); J. Frank and E. Teller, *J. Chem. Phys.* **6**, 861 (1938).

²M. Trlifaj, *Czech. J. Phys.* **6**, 533 (1956); **8**, 510 (1958).

³Th. Förster, *Ann. Phys. (Germany)* **21**, 55 (1948); *Z. Naturforsch.* **4a**, 321 (1949).

⁴D. L. Dexter, *J. Chem. Phys.* **21**, 836 (1953).

⁵O. Simpson, *Proc. Roy. Soc. (London)* **A238**, 402 (1956).

⁶R. C. Powell and R. G. Kepler, *Phys. Rev. Letters* **22**, 636 (1969); **22**, 1232 (1969).

⁷R. C. Powell and R. G. Kepler, *J. Luminescence* **1**, 254 (1969).

⁸R. C. Powell, *Phys. Rev. B* **2**, 1159 (1970).

⁹R. C. Powell, *Phys. Rev. B* **2**, 2090 (1970).

¹⁰R. C. Powell and R. G. Kepler, *Mol. Liquid Crystals* **11**, 349 (1970).

¹¹R. C. Powell, *Phys. Rev. B* **4**, 628 (1971).

¹²J. B. Birks, *J. Luminescence* **1**, 264 (1969). The refutation is in Ref. 9, where thin crystals without reabsorption are studied.

¹³H. B. Rosenstock, *Phys. Rev.* **187**, 1166 (1969). The refutation is in R. C. Powell, *Phys. Rev. B* **2**, 1207 (1970) and consists in observing that only the long-time behavior is explained, whereas it is the short-time behavior that is anomalous.

¹⁴J. B. Birks, *J. Phys. B* **3**, 1704 (1970).

¹⁵R. M. Pearlstein, K. Lakatos-Lindenberg, and R. P. Hemenger, *Phys. Rev. Letters* **27**, 1509 (1971).

¹⁶R. C. Powell and Z. G. Soos, *Phys. Rev. B* **4**, 1547 (1972).

¹⁷See, for example, S. A. Rice and J. Jortner, in *Physics and Chemistry of the Organic Solid State*, edited by D. Fox, M. M. Labes, and A. Weissberger (Interscience, New York, 1967), Vol. III, p. 199. M. Grover and R. Silbey, in *J. Chem. Phys.* **54**, 4843 (1971), conclude that exciton-phonon coupling leads to a hopping motion for the exciton at finite temperatures, provided the exciton band width is sufficiently small. M. R. Philpott [*ibid.* **54**, 111 (1971)] concludes that the anthracene singlet-exciton band width is more than 600 cm^{-1} , which suggests coherent (band) motion. The theoretical situation is thus far from settled.

¹⁸M. Rudemo, *J. Appl. Math.* **14**, 1293 (1966).

¹⁹H. C. Wolf, in *Advances in Atomic and Molecular Physics*, edited by D. R. Bates and J. Estermann (Aca-

demic, New York, 1967), Vol. 3, p. 119.

²⁰(a) A. Propstl and H. C. Wolf, *Z. Naturforsch.* **18a**, 822 (1963); (b) A. Schmillen and J. Kohlmannsperger, *ibid.* **18a**, 627 (1963); (c) A. M. Bonch-Bruevich, B. P. Kovaley, L. M. Belaev, and G. S. Belikova, *Opt. i Spektroskopiya* **11**, 623 (1961) [*Opt. Spectry. (USSR)* **11**, 335 (1961)]; (d) V. L. Zima, A. D. Kravchenko, and A. N. Faidysh, *Opt. i Spektroskopiya* **20**, 441 (1966) [*Opt. Spectry. (USSR)* **20**, 240 (1966)]; (e) A. Schmillen, *Z. Physik* **150**, 123 (1958); (f) A. Schmillen and R. Legler, *Z. Naturforsch.* **18a**, 1 (1963); (g) K. W. Benz and H. C. Wolf, *ibid.* **19a**, 177 (1964); (h) G. Wendell and G. Härtig, *Z. Physik. Chem. (Frankfurt)* **221**, 17 (1962).

²¹F. Spitzer, *Principles of Random Walk* (Van Nostrand, Princeton, N. J., 1964), Chaps. I and VI, see especially pp. 300-301 and 341-342.

²²E. W. Montroll and G. H. Weiss, *J. Math. Phys.* **2**, 167 (1965).

²³Activator-induced host traps, as noted in Ref. 16, are consistent with the PK data.

²⁴A. A. Maradudin, E. W. Montroll, G. H. Weiss, R. Herman, and H. W. Milnes, *Acad. Roy. Belg. Classe. Sci. Mem. Collection in 4°* **2**, 14 (1960), No. 7.

²⁵E. W. Montroll, *J. Math. Phys.* **10**, 753 (1969).

²⁶The derivation follows at once from the fact that $C_n(A)$ plays the same role as $R_n = C_n(0)$ in Eq. (2) of Ref. 18 and that the $n \rightarrow \infty$ limit exists for finite A as well as for $A = 0$.

²⁷R. J. Duffin, *Duke Math. J.* **20**, 233 (1954).

²⁸G. H. Vineyard, *J. Math. Phys.* **4**, 1191 (1963).

²⁹S. Chandrasekhar, *Rev. Mod. Phys.* **15**, 1 (1943).

³⁰P. J. Davis and I. Polonsky, in *Handbook of Mathematical Functions*, edited by M. Abramowitz and I. A. Stegun, Natl. Bur. of Std. Applied Mathematic Series (U. S. GPO, Washington, D. C., 1964), pp. 887 and 919. The $n=28$ weights were kindly provided by H. Rabitz, Department of Chemistry, Princeton University.

³¹The $k(t)$ data shown in Fig. 1 of Ref. 16 were obtained in this way and are more properly interpreted as the $k(t)$ value at the center, rather than at the end, of the 5-nsec time intervals chosen.

³²D. P. Craig and M. R. Philpott, *Proc. Roy. Soc. (London)* **A243**, 213 (1966).

³³D. P. Craig and S. H. Walmsley, *Excitons in Molecular Crystals* (Benjamin, New York, 1968), pp. 127-132.

³⁴T. R. Waite, *Phys. Rev.* **107**, 463 (1957).

³⁵M. Yokota and O. Tanomoto, *J. Phys. Soc. Japan* **22**, 779 (1967); Y. A. Kurskii and A. S. Selivanenko, *Opt. i Spektroskopiya* **8**, 643 (1960) [*Opt. Spectry. (USSR)* **8**, 340 (1960)].